Research Square

Preprints are preliminary reports that have not undergone peer review.
They should not be considered conclusive, used to inform clinical practice,
or referenced by the media as validated information.

KLK5 overexpression predicts poor prognosis and promotes migration and adhesion in non-small cell lung cancer

Adriana Stuardo-Parada
Austral University of Chile
Carlos D. Figueroa
Austral University of Chile
Larissa Turones
Austral University of Chile
Cinthia Mella Robles
Austral University of Chile
Pía Bascur
Austral University of Chile
Francisca Pavicic
Austral University of Chile
Claudia Torres-Farfán
Austral University of Chile
Rodrigo López
Austral University of Chile
Franz Villarroel-Espindola
INCLIVA Health Research Institute
Tobias Dreyer
Technical University of Munich
Viktor Magdolen
Technical University of Munich
Pamela Ehrenfeld
ingridehrenfeld@uach.cl

Austral University of Chile

Research Article

Keywords: KLK5, Non-small cell lung cancer, Lung adenocarcinoma, Cell migration, Prognostic biomarker

Posted Date: September 22nd, 2026

DOI: https://doi.org/10.21203/rs.3.rs-10133408/v1

License: This work is licensed under a Creative Commons Attribution 4.0 International License.
Read Full License

Additional Declarations: No competing interests reported.

KLK5 overexpression predicts poor prognosis and promotes migration and adhesion in non-small cell lung cancer

Adriana Stuardo-Parada[1,2], Carlos D. Figueroa[1,3], Larissa Turones[1,4], Cinthia Mella Robles[1,4], Pía Bascur[1,5], Francisca Pavicic[1,4], Claudia Torres-Farfan[4,6], Rodrigo López[4,7], Franz Villarroel-Espindola[8], Tobias Dreyer[9], Viktor Magdolen[9] and Pamela Ehrenfeld[1,4*]

1. Laboratory of Cellular Pathology, Institute of Anatomy, Histology and Pathology, Faculty of Medicine, Universidad Austral de Chile, Valdivia, Chile
2. Faculty of Dentistry, Universidad San Sebastián, Valdivia, Chile
3. The Kallikrein House, Valdivia, Chile
4. Center for Interdisciplinary Studies on Nervous System (CISNe), Universidad Austral de Chile, Valdivia, Chile
5. Fundación Arturo López Pérez (FALP) Cancer Center, Santiago, Chile
6. Laboratory of Developmental Chronobiology, Institute of Anatomy, Histology and Pathology, Faculty of Medicine, Universidad Austral de Chile, Valdivia, Chile
7. Institute of Pharmacy, Faculty of Sciences, Universidad Austral de Chile, Valdivia, Chile.
8. INCLIVA Health Research Institute (Cancer), Valencia, Spain.
9. Department of Gynaecology and Obstetrics, Technical University of Munich, Munich, Germany

Running title: KLK5 promotes migration and adhesion in NSCLC cells

***Correspondence:** Pamela Ehrenfeld, ingridehrenfeld@uach.cl

ORCID

Adriana Stuardo-Parada https://orcid.org/0000-0003-3578-7125

Larisa Turones https://orcid.org/0000-0003-4646-5682

Pamela Ehrenfeld https://orcid.org/0000-0002-2519-7570

Abstract

Background Kallikrein-related peptidase 5 (KLK5) is a secreted serine protease involved in extracellular matrix remodeling and proteolytic signaling, but its role in non-small cell lung cancer (NSCLC) remains poorly understood. **Methods** The association between KLK5 expression and patient survival was first evaluated in silico in publicly available NSCLC datasets using the Kaplan–Meier Plotter platform, stratified by overall and progression-free survival and by histological subtype. Functional effects were then examined in vitro in the lung adenocarcinoma cell line A549, using stable KLK5-overexpressing clones, an empty-vector control, and stimulation with exogenous recombinant KLK5 (rKLK5). Migration was assessed by Transwell assays, adhesion to extracellular matrix components (including collagen I and fibronectin) by adhesion assays, and proliferation and cisplatin sensitivity by cell viability assays. Epithelial–mesenchymal transition (EMT) markers (E-cadherin, N-cadherin, and vimentin) and the effect of cisplatin on KLK5 expression were evaluated by quantitative PCR, ELISA, Western blot, and immunofluorescence. **Results** High KLK5 expression was significantly associated with shorter overall and progression-free survival, particularly in lung adenocarcinoma, supporting its potential value as a prognostic biomarker. In A549 cells, both KLK5 overexpression and exogenous recombinant KLK5 significantly increased cell migration and adhesion to collagen I and fibronectin, while no effects were observed on proliferation or cisplatin sensitivity. Importantly, these changes occurred in the absence of a canonical epithelial–mesenchymal transition, as no consistent alterations were detected in epithelial or mesenchymal protein markers. Cisplatin exposure increased KLK5 mRNA expression without a corresponding increase in protein levels, suggesting post-transcriptional regulation under treatment-induced stress. **Conclusions** KLK5 represents a clinically relevant prognostic biomarker in NSCLC that promotes a

motile and adhesive tumor cell phenotype through an epithelial–mesenchymal transition-independent mechanism. The differential effects observed between endogenous and exogenous KLK5 indicate a context-dependent role for this protease, supporting its further evaluation as a biomarker and potential therapeutic target in lung cancer.

Keywords: KLK5, Non-small cell lung cancer, Lung adenocarcinoma, Cell migration, Prognostic biomarker

Introduction

Lung cancer is the most diagnosed cancer worldwide in men and the second in women, with an estimated 2.5 million new cases and 1.8 million deaths annually, making it the leading cause of cancer-related mortality [1,2]. Histologically, lung cancer is classified into small-cell lung carcinoma (SCLC, 15%) and non-small cell lung cancer (NSCLC, 85%) [3]. Despite advances in diagnosis and treatment, the 5-year survival rate remains low in most countries, ranging from 10% to 20%, largely because many patients are diagnosed at advanced stages and therapeutic options remain limited [4,5].

Treatment selection in NSCLC depends on tumor histology, disease stage, and patient condition [6]. Although targeted therapies have improved outcomes in selected molecular subgroups, fewer than 25% of patients derive sustained benefit, and resistance remains a major clinical challenge. For most patients, platinum-based chemotherapy continues to represent a cornerstone of treatment despite frequent intrinsic or acquired chemoresistance and substantial toxicity. Tumor progression and therapeutic failure in NSCLC are increasingly recognized as consequences of tumor cell plasticity, including alterations in cell–matrix interactions and adaptive changes that enhance survival and dissemination [7–9].

Epithelial–mesenchymal transition (EMT) has been widely studied as one mechanism underlying this plasticity. During EMT, epithelial tumor cells lose cell–cell adhesion and acquire a more motile phenotype, commonly accompanied by reduced E-cadherin expression and increased mesenchymal markers such as N-cadherin and vimentin. EMT has also been associated with treatment resistance and poor clinical outcome in NSCLC [10–12]. Recent evidence in NSCLC indicates that tumor cells may acquire invasive and therapy-resistant phenotypes through intermediate epithelial–mesenchymal states rather

than through a complete canonical EMT program, suggesting that additional molecular regulators contribute to tumor progression [13,14].

Kallikrein-related peptidase 5 (KLK5) is a secreted serine protease belonging to the human kallikrein family, several members of which have been associated with either favorable or poor prognosis in lung cancer [15]. KLK5 was first identified in the human epidermis, where it plays a critical role in desquamation through cleavage of corneodesmosomal proteins [16]. In addition, KLK5 can degrade several extracellular matrix components (ECM), including collagens, fibronectin, and laminin, and can activate other pro-Kallikreins [17,18]. In the respiratory tract, KLK5 has been implicated in basal layer degradation in chronic obstructive pulmonary disease and has been shown to promote EMT in bronchial epithelial cells [19]. Because KLK5 can modify extracellular matrix composition, it may influence tumor cell interactions with the microenvironment and thereby regulate cell motility.

Although KLK5 has previously been proposed as a prognostic biomarker in NSCLC, its functional role in tumor progression remains incompletely understood. To address this, in silico survival analyses were combined with in vitro functional approaches to evaluate the prognostic relevance of KLK5 in NSCLC and to determine whether KLK5 regulates tumor cell migration, adhesion, proliferation, and cisplatin response independently of canonical epithelial–mesenchymal transition. These findings provide additional insight into the potential relevance of KLK5 in disease progression and treatment response, supporting its further evaluation as a biomarker and potential therapeutic target in lung cancer.

Materials and methods

Differential expression of KLK5 and its relationship with prognosis

To explore the association between KLK5 gene expression and its prognostic value in an NSCLC cohort, the Kaplan–Meier Plotter online database (KM Plotter; http://kmplot.com; last accessed March 20, 2025) [20] was used. This bioinformatics platform is designed to assess the association between gene expression and patient survival by generating Kaplan-Meier survival curves for selected patient cohorts. In this study, patients were stratified according to the median expression of KLK5 (Affymetrix ID 222242_s_at) using all available probe sets per gene while excluding biased arrays. Survival curves were generated to compare low versus high KLK5 expression in relation to overall survival (OS) and progression-free survival (PFS) in the NSCLC cohort. Hazard ratios (HRs) with corresponding 95% confidence intervals (CIs) and log-rank P values were recorded.

Cell culture and cell transfection

The A549 cell line (ATCC CCL-185) derived from lung adenocarcinoma was obtained from ATCC (Virginia, USA). Cells were cultured in RPMI-1640 medium (Cytiva, USA) supplemented with 10% heat-inactivated fetal bovine serum (Cytiva, USA), 1% penicillin-streptomycin (Cytiva, USA), and 250 mg/mL amphotericin B (Biological Industries, Israel). Cells were maintained at 37 °C in a humidified incubator under 5% CO_2. The pRC-RSV vector plasmid was purchased from OriGene Technologies (USA). Three hundred thousand A549 cells were seeded in a 6-well plate and grown until they reached 80% confluence. Cells were then starved in serum-free medium for 24 h before transfection with pRC-RSV-KLK5 or the empty control vector (pRC-RSV). For each well, 12 µL of Lipofectin (Invitrogen, USA) and 6 µg of DNA were used for transfection. Cell clones incorporating pRC-RSV were selected by adding 1 mg/mL neomycin (Life Technologies, USA) to the

culture medium. After one week, single-cell clones were isolated by trypsinization and seeded individually into 24-well plates. Overexpression was confirmed by qPCR.

Additionally, cisplatin (Pfizer, USA) was used at a final concentration of 10 µM, a concentration found in the plasma of cancer patients receiving chemotherapy [21]. Whereas recombinant KLK5 (rKLK5, 1108-SE, R&D Systems, USA) was applied at final concentrations of 20, 50, and 100 ng/mL in the corresponding stimulation experiments.

qPCR

Total RNA was extracted from cell extracts using the RNeasy kit (Qiagen, Germany). The concentration of isolated mRNA was determined by measuring 1 µL of each sample with a NanoDrop spectrophotometer. To evaluate potential contamination, 260/280 nm and 230/260 nm absorbance ratios were measured. Samples with values between 1.8 and 2.0 were considered high quality and stored at –80 °C. cDNA synthesis was performed with 1 µg of total RNA using the RevertAid First Strand cDNA Synthesis Kit (Thermo Fisher Scientific, USA). Quantitative PCR analysis was performed with 150 ng of cDNA per well using Biozym Blue Probe qPCR Mix (Biozym Scientific GmbH, Germany) and TaqMan Probe (Thermo Fisher Scientific, USA) for the following targets: KLK5 (Hs01548153_m1), E-cadherin 1 (Hs01023895_m1), N-cadherin 2 (Hs00983056_m1), Vimentin (Hs00958111_m1), and housekeeping gene HPRT1 (Hs02800695_m1). Threshold cycles (Ct) were used to calculate the level of gene expression relative to the housekeeping gene HPRT1, using the $2^{-\Delta Ct}$ method [22]. All kits were used according to the manufacturer's instructions.

Enzyme-Linked Immunosorbent Assay (ELISA)

KLK5 levels were measured in cell extracts and conditioned media using a commercially available human KLK5 sandwich ELISA kit (ab131555, Abcam, UK), according to the manufacturer's instructions. Cell extracts were prepared as described for Western blot analysis. Protein samples were standardized to 40 µg using the sample diluent buffer provided. Conditioned media were centrifuged to remove cell debris, and 100 µL of the supernatant was added to each well. Absorbance was measured at 450 nm using a Multiskan FC microplate reader (Thermo Fisher Scientific, USA).

Cell proliferation assay

Cell proliferation was assessed using the CellTiter-Glo Viability Assay (Promega, USA) according to the manufacturer's instructions. A549 cells were seeded in opaque 96-well plates at a density of 1.5×10^3 cells per well, cultured for 24 h, and then stimulated with recombinant KLK5 (rKLK5, 1108-SE, R&D Systems, USA) at 20, 50, and 100 ng/mL. Additionally, the proliferation of A549 clones was assessed after 24 h of growth. Luminescence was measured using a Victor X2 multilabel plate reader (PerkinElmer, USA).

MTT and Crystal violet

MTT was diluted and filtered in RPMI-1640 to 1 mg/mL. Cells were incubated with 100 µL for 3.5 h, after which the medium was removed, and formazan crystals were solubilized with 100 µL of HCl-isopropanol. Background absorbance was measured using cell-free control wells. Absorbance was read at 560 nm using a Multiskan FC microplate reader (Thermo Fisher Scientific, USA). For the crystal violet assay, a 0.5% solution was prepared by dissolving 0.5 g of dye in 80 mL of distilled water and adding 20 mL of methanol. Cells

were fixed with crystal violet for 20 min at 4°C and washed three times with PBS. Independent experiments were made in triplicate.

Immunofluorescence

Cells were seeded on 12 mm diameter coverslips in 24-well plates. After the corresponding treatments or stimuli, cells were fixed with 4% paraformaldehyde (PFA) for 10 min at 37 °C, and then they were thoroughly washed with PBS and permeabilized with 0.2% Triton X-100 for 30 min at room temperature and blocked with 5% FBS for 30 min at room temperature. Next, the cells were incubated with anti-KLK5 antibody (ab7283, Abcam, UK) at 1:100 dilution in a humid chamber for 1 h at 37 °C. Following washing with PBS, they were incubated with an AlexaFluor568-labeled anti-rabbit secondary antibody (A10042, Thermo Fisher Scientific, USA) at 1:1000 dilution, and nuclei were stained with DAPI (1:10.000) for 1 h at 37 °C. When cells were treated with brefeldin A, it was added directly to the culture media during the last 3 h of culture. Coverslips were mounted on glass slides using Dako fluorescence mounting medium (Thermo Fisher Scientific, USA). Negative controls were prepared by replacing the primary antibody with PBS and 0.5% BSA.

Western blotting

Cells were lysed in RIPA buffer (50 mM Tris-HCl, pH 7.4; 150 mM NaCl; 0.25% deoxycholic acid; 1% Nonidet P-40; 1 mM EDTA) supplemented with protease and phosphatase inhibitors. Lysates were incubated on ice for 30 min and centrifuged at 18,000 × g for 20 min at 4 °C. Protein concentration was determined using the Pierce™ BCA Protein Assay Kit (Thermo Scientific™). Equal amounts of protein (30 µg) were separated by 10% SDS-PAGE under denaturing conditions and transferred onto nitrocellulose

membranes (0.45 µm). Membranes were probed with primary antibodies against vimentin (#5741), N-cadherin (#13116), E-cadherin (#3195), and GAPDH (Cell Signaling Technology, USA). Protein bands were detected using SuperSignal™ West Dura Chemiluminescent Substrate (Thermo Scientific™) and visualized with an iBright Imaging System (Thermo Scientific™).

Transwell migration assay

The migratory ability of lung cancer cells was assessed using 24-well Transwell inserts with 8.0 µm pore polycarbonate membranes (Corning Life Sciences, USA). A549 wild-type cells were seeded in 6-well plates and stimulated for 24 hours with rKLK5 at different concentrations. Both the rKLK5-stimulated A549 cells and the A549 clones were cultured overnight in 35 mm plates and subsequently trypsinized. A total of 1.5×10^4 cells in 300 µL of serum-free medium were added to the upper chamber of the insert, which was placed in a 24-well plate containing 700 µL of medium with 10% FBS in the lower chamber. After overnight migration, the membranes were fixed with 0.5% crystal violet, and images were captured using an optical microscope at 100× magnification with a digital camera. Cell migration was quantified by counting the number of cells in 16 fields per membrane.

ECM adhesion assay

The cell adhesion assay was performed using the colorimetric CytoSelect Cell Adhesion Assay Kit (CBA-070, Cell Biolabs, Inc., USA), following the manufacturer's instructions. Briefly, cells were harvested and resuspended in serum-free RPMI 1640 medium, then seeded onto ECM-coated wells (fibronectin, collagen I, collagen IV, fibrinogen, laminin I) and BSA-coated wells as a negative control, at a density of 1.15×10^5 viable cells per well,

in triplicate. The plates were incubated for 90 min at 37 °C to allow cell adhesion. Following incubation, the medium was carefully removed, and wells were gently washed with PBS to eliminate non-adherent cells. Adherent cells were stained for 10 min at room temperature, after which the wells were washed with deionized water. Subsequently, 200 µL of extraction solution was added to each well, followed by 10 min incubation in a shaker at room temperature. Finally, 150 µL of the resulting solution from each well was transferred to a 96-well microplate, and absorbance was measured at 560 nm using a Multiskan FC microplate reader (Thermo Fisher Scientific, USA).

Graphics and statistical analysis

Statistical analyses were performed using GraphPad Prism. Data distribution was assessed using the Shapiro–Wilk normality test prior to group comparisons. For normally distributed data, comparisons between two groups were performed using a two-tailed unpaired Student's t-test, whereas comparisons among more than two groups were analyzed using one or two way analysis of variance (ANOVA) followed by Tukey's multiple-comparison test when appropriate. Differences were considered statistically significant at $p \leq 0.05$. All data are presented as mean ± SEM. Unless otherwise indicated, n represents three independent biological replicates derived from separate cell passages.

Results

KLK5 overexpression predicts poor overall and progression-free survival in NSCLC, particularly lung adenocarcinoma

Publicly available datasets were analyzed using Kaplan-Meier Plotter. KLK5 gene expression is significantly associated with poorer overall survival (OS) (Fig. 1a; HR = 1.3, *P*

< 0.001) and poor progression-free survival (PFS) (Fig. 1b; HR = 1.76, *P* < 0.001) in patients with NSCLC. Similarly, in the lung adenocarcinoma subset (LUAD), elevated KLK5 expression remained significantly associated with poorer OS (Fig. 1c; HR = 1.47, *P* < 0.001) and showed an even stronger association with poorer PFS (Fig. 1d; HR = 2.31, *P* < 0.001). In the lung squamous cell carcinoma (SCC) subset, KLK5 expression showed a weaker association with OS (Fig. 1e; HR = 1.36, *P* = 0.0017), whereas no significant association was observed for PFS (Fig. 1f; HR = 1.17, *P* = 0.46).

Validation of the KLK5 overexpression cell model

To assess the impact of KLK5 on lung cancer cells, A549 cells were transfected with a KLK5 expression plasmid, generating several clones with different levels of KLK5 expression. For subsequent analyses, clone 1 (High-KLK5) and clone 7 (Low-KLK5) were selected, along with the empty vector control (Ev) and wild-type cells (Wt) (Fig. 2a). Transfection stability was confirmed by qPCR analysis across four different passages for each clone. KLK5 expression in the High-KLK5 clone was significantly higher than in wild-type, empty vector, and Low-KLK5 cells (Fig. 2b, $p<0.01$).

KLK5 protein levels were analyzed in the selected clones, both in cell extracts and in conditioned culture media. In cell extracts (Fig. 2c), the High-KLK5 clone (0.29 ng/mL) exhibited significantly higher protein levels compared to Wt (0.12 ng/mL), Ev (0.13 ng/mL) ($p<0.01$), and Low-KLK5 (0.07 ng/mL) ($p<0.01$). In conditioned media (Fig. 2d), KLK5 protein levels in the High-KLK5 clone reached a mean value of 3.75 ng/mL, significantly higher than those observed in Wt, Ev, and Low-KLK5 clones (0.24 ng/mL) ($p<0.0001$), consistent with the gene expression data (Fig. 2b).

KLK5 does not alter the growth of lung cancer cells

Cell proliferation was assessed using the CellTiter-Glo assay, a luminescence-based kit that quantifies ATP as a marker of metabolically active cells. A549 cells were seeded and cultured for 24 hours, then stimulated with recombinant KLK5 (rKLK5) at concentrations of 20, 50, and 100 ng/mL for an additional 24 hours. A549 clones were also seeded, and the assay was performed 24 hours later. Since the fetal bovine serum (FBS) content in the culture medium can influence cell proliferation, experiments were conducted under both 1% and 10% FBS conditions. No significant differences in cell growth rates were observed in A549 clones (Fig. 3a, 3b) or in A549 cells treated with rKLK5, regardless of the concentration used (Fig. 3c, 3d). As expected, the proliferation rate was higher under 10% FBS; however, no significant differences were detected between rKLK5-stimulated and non-stimulated cells under either condition. These findings were corroborated by an MTT assay conducted over a 96-hour period. A linear correlation between cell number and absorbance was confirmed for each clone, and the mean growth rate constant (k) did not differ significantly among groups ($p = 0.34$) (Fig. S1).

Cisplatin induces KLK5 mRNA expression without a corresponding increase in secreted protein levels

The effect of cisplatin on KLK5 expression was evaluated in A549 cells following a 48 h treatment with 10 μM cisplatin. As shown in Fig. 4a, cisplatin significantly increased KLK5 gene expression compared to untreated controls, determined by qPCR ($p<0.01$). Surprisingly, no significant increase in KLK5 protein levels was observed by ELISA in the same group (Fig. 4b).

Immunofluorescence revealed cytoplasmic localization of KLK5, with increased staining intensity following 10 μM cisplatin treatment. Given that kallikreins are typically secreted proteins, their presence in the cytoplasm is consistent with their role in the secretory pathway. This hypothesis is further supported by the increased immunofluorescence signal observed upon treatment with Brefeldin A. This drug indirectly inhibits protein transport from the endoplasmic reticulum to the Golgi apparatus by preventing COP-I coat association with the Golgi membrane (Fig. 4c).

Additionally, conditioned media from the same experimental groups were analyzed to evaluate secreted KLK5 levels; however, KLK5 protein was not detected by the ELISA assay.

KLK5 expression does not alter cisplatin sensitivity in A549 cells

Given that KLK5 expression increased after cisplatin treatment in wild-type A549 cells, the susceptibility of A549 clones to this chemotherapeutic agent was analyzed by determining the IC_{50} values for each clone. After 48 h of treatment, the IC_{50} values were 6.9 ± 1.9 μM for wild-type (Wt) cells, 9.8 ± 4 μM for the empty vector (Ev) control, 5.3 ± 4 μM for the Low-KLK5 clone, and 6.9 ± 4.6 μM for the High-KLK5 clone. No significant differences were observed between clones (Fig. 5a). Cell viability following cisplatin treatment was also assessed under the microscope using crystal violet, as illustrated in Fig. 5b. These results indicate that the sensitivity to cisplatin is not affected by different KLK5 expression levels.

KLK5 increases migration of A549 lung cancer cell

The effect of KLK5 on cell migration was evaluated using a Transwell migration assay. A549 clones were allowed to migrate overnight, and the High-KLK5 clone exhibited significantly higher migration compared to wild-type (Wt) and empty vector (Ev) control (Fig. 6a, $p<0.01$). Additionally, A549 cells were stimulated with recombinant KLK5 (rKLK5) at concentrations of 20, 50, and 100 ng/mL. After overnight migration, treatment with 100 ng/mL rKLK5 significantly increased cell migration compared to 0 and 20 ng/mL (Fig. 6b, $p<0.05$).

KLK5 does not induce a canonical EMT program in A549 clones

EMT is a biological process in which epithelial cells modify their phenotype to acquire a more migratory and invasive phenotype. Among the main reported changes, EMT is characterized by reducing the levels of E-cadherin and increasing the expression of mesenchymal markers, such as N-cadherin and vimentin. To evaluate EMT status, the expression of these markers in the different A549 clones was analyzed. The High-KLK5 clone exhibited a significant decrease in E-cadherin gene expression compared to clones lacking KLK5 expression ($p<0.05$) and a significant reduction in N-cadherin gene expression ($p<0.05$). In contrast, vimentin gene expression did not differ significantly between clones (Fig. 7a). Nevertheless, no significant differences in protein levels were observed for any of these markers relative to wild-type or empty vector controls, as determined by Western blotting (Fig. 7b).). Notably, the transcript-level changes in E- and N-cadherin did not follow the reciprocal pattern of a classical cadherin switch and were not accompanied by concordant protein-level changes, indicating that the KLK5-associated migratory phenotype is not explained by a canonical EMT program.

The expression of EMT markers at the mRNA and protein levels was also evaluated following stimulation of A549 lung cancer cells with 20, 50, and 100 ng/mL of recombinant rKLK5. Both E-cadherin and N-cadherin gene expression showed a decreasing trend with increasing rKLK5 concentrations, but none of the changes were statistically significant (Fig. 8a). At the protein level, no significant changes were observed in response to different concentrations of rKLK5, confirming that the differences in gene expression were not reflected at the protein level (Fig. 8b). These results indicate that changes in classical EMT markers do not fully explain the increased migratory capacity observed in A549 lung cells.

KLK5 enhances adhesion of lung cancer cells to select ECM components.

Based on the increased cell migration observed in response to 100 ng/mL of rKLK5 and in the High-KLK5 clone, it was hypothesized that KLK5 may alter the affinity of cells for specific ECM components, thereby modulating cell adhesion. Adhesion assays revealed that the High-KLK5 clone exhibited significantly greater adhesion to collagen I compared to controls (Fig. 9a, $p<0.05$). Additionally, stimulation with 100 ng/mL rKLK5 enhanced the adhesion of wild-type A549 lung cancer cells to both fibronectin and collagen I after 90 minutes of incubation (Fig. 9b, $p<0.05$). By contrast, adhesion of both A549 clones and wild-type A549 cells to laminin I and fibrinogen was minimal (Figs. 9a, 9b). These results indicate a consistent pattern in the differential affinity of cells toward specific ECM components.

Discussion

Using an online database, the association between KLK5 tumor expression and patient survival was validated in a larger NSCLC cohort. In light of evidence linking KLK5 to poor

prognosis in lung cancer, its potential contribution to a more aggressive phenotype was then assessed by examining EMT, migration, proliferation, adhesion to selected ECM components, and cisplatin response in vitro.

KLK5 was originally identified in the human epidermis, where it plays a key physiological role in skin homeostasis by mediating desquamation through proteolytic cleavage of corneodesmosomal proteins [16]. Beyond this function, KLK5 exhibits broad proteolytic activity, degrading extracellular matrix components such as collagens, fibronectin, and laminin, and also activating other KLKs [17,18]. These properties highlight KLK5 as a multifunctional protease involved in tissue remodeling and dynamic regulation of the extracellular environment.

In-silico analyses of publicly available datasets showed that high KLK5 expression was significantly associated with shorter overall and progression-free survival in NSCLC, particularly in lung adenocarcinoma, supporting its role as a poor prognostic marker. This is consistent with previous reports linking increased serum KLK5 levels to unfavorable survival and poorer response to anlotinib [23], further supporting its clinical relevance as a biomarker of aggressive disease in NSCLC.

Because high KLK5 expression was associated with adverse clinical outcomes, whether this could reflect enhanced tumor cell proliferation was assessed. However, neither rKLK5 nor stable KLK5 overexpression altered proliferation in the present model, suggesting that KLK5 does not directly regulate proliferation in lung adenocarcinoma cells. Although KLK5 silencing reportedly reduces proliferation in PC-9 cells [24], these findings indicate that its prognostic impact is unlikely to depend mainly on proliferative mechanisms.

Instead, the association between high KLK5 expression and adverse outcome may reflect its involvement in other tumor-promoting processes, including migration and epithelial–mesenchymal transition. Consistently, higher circulating KLK5 levels have been linked to reduced response to anlotinib [23], suggesting a more invasive and treatment-refractory phenotype. Together, these findings indicate that KLK5 may contribute to NSCLC progression beyond effects on cell growth.

Likewise, no significant proliferative changes were observed in the KLK5 loss- or gain-of-function models. Consistent with this, studies in other cancer models have shown that KLK5 silencing alters migratory and invasive behavior without affecting proliferation, including in human gastric cancer cell lines [25], and in the urinary bladder carcinoma cell line Ku1 [25]. Similarly, KLK5 silencing reduced proliferation and migration in oral squamous carcinoma cells, consistent with evidence linking a higher KLK5/SPINK5 (LEKTI) ratio to poorer prognosis. This suggests that an imbalance between KLK5 and its endogenous inhibitor, rather than LEKTI levels alone, may underlie a more aggressive phenotype [26]. Although KLK5 has been implicated in several cancer types, current evidence, including the present findings, indicates that it does not significantly affect cell proliferation, suggesting a limited role in this process.

In the present model, 48 h of cisplatin treatment increased KLK5 mRNA expression without a significant change in protein levels. Similar induction of KLK5 transcripts has been reported in breast (BT-20) and androgen-independent prostate cancer (DU145) cells following exposure to epirubicin, docetaxel, methotrexate, and mitoxantrone [27,28]. In prostate PC3 cells, KLK5 was also induced by chemotherapy, although the extent of induction varied by agent and exposure time, with carboplatin causing a delayed increase

compared with other drugs [29]. Together, these observations suggest that KLK5 upregulation may be part of a broader response to cytotoxic stress, although its extent appears to vary across tumor types and treatment conditions. Supporting this view, stress-induced regulation has also been described for other kallikrein-related peptidases [30].

No direct effect of cisplatin on KLK5 protein expression was detected in the present assays, suggesting that its regulation may occur secondary to broader cytotoxic stress responses. These responses may involve rapid miRNA-mediated regulation and more sustained epigenetic mechanisms. Supporting this possibility, cisplatin modulates KLK13 expression in esophageal and gastric cancer models through context-dependent mechanisms that may involve TET2/3-associated demethylation or be independent of it [31,32]. Given its multiple CpG islands [33], KLK5 may be subject to epigenetic regulation. In silico analyses also identify it as one of the most miRNA-targeted KLKs, with predicted regulators such as miR-106b, miR-125a, and miR-143 [34] which are deregulated in lung cancer and linked to EMT, DNA repair, and drug resistance [35–38]. These miRNAs may also influence cisplatin responsiveness by modulating drug transporters and survival pathways, in addition to potentially regulating KLK5 [39]. Together, these findings suggest that cisplatin-induced changes in KLK5 expression may involve both miRNA-dependent and epigenetic mechanisms.

Although KLK5 protein was detected by ELISA, KLK5 mRNA was expressed at very low levels in wild-type A549 cells at baseline, near the detection limit of the assay. This basal level was markedly lower than that of the KLK5-overexpressing clones and is therefore barely distinguishable from zero on the scale of Fig. 2b; nevertheless, it remained quantifiable and was significantly increased by cisplatin treatment (Fig. 4a). To mimic the

increase that may follow cisplatin treatment, KLK5-overexpressing A549 cells were generated by plasmid transfection. The High-KLK5 clone showed markedly higher KLK5 mRNA and protein levels than wild-type cells, the empty-vector control, and the Low-KLK5 clone, in both cell extracts and conditioned media. Although KLK5 transcripts are annotated in A549 cells, only a very low signal was detected with the TaqMan assay. Given that KLK5 has at least five annotated splice variants (HGNC:6366; ENSG00000167754), of which only four include the sequence targeted by the primers and probe used, A549 cells may also express variants outside this amplicon, such as KLK5-204 with an alternative 5′-UTR, so that the amplicon-targeted assay likely captures only part of the total KLK5 transcript pool and underestimates its overall abundance. This may also contribute to the apparent uncoupling between low measured KLK5 mRNA and detectable secreted protein. The functional significance of these variants remains unclear. Previous studies have also described heterogeneous KLK5 transcript profiles across cancer types, including variants with altered 5′-UTRs or truncated coding regions that may generate shorter, less readily secreted proteins [40–43]. Such transcript and protein form diversity is a recognized feature of the KLK family and complicates molecular characterization. Nevertheless, the robust KLK5 expression in the overexpressing clones confirms successful transfection and supports downstream functional analyses.

Cell migration is a central mechanism of metastatic dissemination. In the present assays, exogenous rKLK5 increased migration of wild-type A549 cells in a dose-dependent manner, and High-KLK5 clones displayed greater migratory capacity than wild-type and Low-KLK5 cells.

Mechanistically, KLK5 may enhance migration through multiple proteolytic pathways, including autocrine degradation of cell–cell adhesion structures, as reported for desmosomal proteins [16,17]. In addition, KLK5 may activate other kallikrein-related peptidases, including KLK7 and KLK14, thereby amplifying proteolytic cascades involved in tumor progression [44]. KLK5 has also been linked to broader protease networks involving matrix metalloproteinases (MMPs), further promoting invasion [45]. Moreover, it can directly degrade extracellular matrix components such as fibronectin, laminin, and collagen [18,45], facilitating tissue remodeling and enhancing cell motility.

Beyond its proteolytic activity, KLK5 may also modulate cell behavior through receptor-mediated signaling. Previous studies have shown that it activates downstream pathways linked to increased migration and inflammatory responses [46,47], although alternative receptor-independent mechanisms have also been described [48]. Although some of these pathways have been linked to EMT-like phenotypes, these were not observed in the present model. Thus, the increased migration observed in High-KLK5 clones and following exogenous rKLK5 stimulation supports a promigratory role for KLK5, likely mediated by combined proteolytic and context-dependent signaling mechanisms rather than by a canonical EMT program.

EMT is typically defined by reduced epithelial adhesion and increased expression of mesenchymal markers, often referred to as the cadherin switch. Here, the effects of KLK5 on migration, together with its modulation of EMT-related markers, suggest that it may promote tumor progression by altering epithelial–mesenchymal plasticity. However, as these promigratory effects were not fully explained by changes in individual EMT markers, the underlying mechanisms remain unclear [49,50].

Lung cancer cell lines often exhibit high invasiveness, reduced E-cadherin expression, and increased resistance to chemotherapeutic agents like cisplatin [51]. As noted above, elevated KLK5 expression did not induce canonical EMT-like changes in any clone, but was associated with downregulation of both E- and N-cadherin mRNA. This was unexpected, since reduced E-cadherin is typically accompanied by increased N-cadherin expression—a cadherin switch that promotes migration and invasion. This process may involve either full replacement or coexistence, with aberrant N-cadherin expression altering cell behavior despite the retention of E-cadherin [52]. Although N-cadherin is commonly linked to increased motility, the present findings indicate that KLK5-driven migration cannot be explained solely by changes in this adhesion molecule. This suggests that KLK5 may act through broader effects on cell–cell adhesion or through additional signaling pathways beyond cadherin regulation. Further studies are needed to define the underlying mechanisms.

The effects of exogenous active rKLK5 may differ from those of endogenously produced KLK5, as suggested by the differential expression of EMT markers. This may reflect the inability of recombinant protein added to the medium to fully recapitulate the biochemical properties of KLK5 secreted by overexpressing cells. Given that KLK5 is highly glycosylated, differences in post-translational modifications, particularly glycosylation, between recombinant and cell-derived protein may influence its activity, stability, or interactions [53]. In addition, while the extracellular functions of KLK5 are well characterized, its potential intracellular activity remains poorly understood.

Cell migration is a key process by which normal and cancer cells traverse the ECM through interactions between ECM components and specific cell-surface molecules. KLK5 may

regulate the ECM and cell adhesion both directly, through its proteolytic activity, and indirectly, through miRNA-mediated mechanisms [54]. Thus, KLK5 dysregulation may reshape miRNA networks and downstream signaling pathways, ultimately affecting invasiveness, metastasis, and patient survival.

Findings from this isolated KLK5-overexpressing cell system support the association between elevated KLK5 expression and reduced OS and PFS in NSCLC, consistent with a role in promoting a more motile phenotype. Altered cell adhesion, partly driven by ECM remodeling, is a hallmark of cancer linked to tumor progression, metastasis, and drug resistance [55,56]. In line with this, KLK5 increased adhesion to collagen I and fibronectin in both High-KLK5 clones and rKLK5-treated wild-type A549 cells.

In lung cancer, increased collagen I is associated with poorer outcomes, including shorter survival, higher relapse risk, and enhanced tumor cell colonization and growth [57,58]. Fibronectin is likewise upregulated in NSCLC, where it promotes tumor progression by enhancing EMT, stemness, and cancer cell migration and invasion [10,56,59]. KLK5 proteolyzes several ECM components, including collagen I, fibronectin, and desmosomal proteins [16,42]. Consistently, KLK5 inhibition or silencing increases adhesion in oral carcinoma cells, whereas its overexpression promotes cell dispersal [60], supporting a role in ECM remodeling and tumor cell motility. Together, these findings support a role for KLK5 in regulating migration and adhesion through an EMT-independent mechanism in NSCLC progression.

Further studies are needed to establish the utility of KLK5 as a predictive or diagnostic biomarker and to clarify its role in lung cancer progression, including chemoresistance and invasiveness, particularly in lung adenocarcinoma. Recent development of SFTI-1-derived

peptide inhibitors with high selectivity for KLK5 [61,62] together with a dual inhibitory antibody against KLK5/KLK7 [63]. highlights the therapeutic potential of targeting this protease family. These findings support KLK5 as a promising therapeutic target in lung cancer.

Declarations

Ethics statement

No ethical approval was required for this study. Kaplan–Meier survival analyses were performed using publicly available datasets, and no identifiable human data were used. All experimental procedures were conducted in vitro using established cell lines.

Availability of data and materials

The survival analyses were performed using publicly available datasets accessed through the Kaplan–Meier Plotter platform (https://kmplot.com). All other data and materials generated during the study are available from the corresponding author upon reasonable request.

Competing interests

The authors confirm that they have no conflict of interests.

Funding

This work was supported by grants FONDECYT 1201635 (PE) and National Doctoral Scholarship 21201493 (ASP) from the National Agency for Research and Development (ANID, Chile).

Author contributions

A.S.-P. conceived and designed the study, performed the experiments, analyzed the data, and wrote the manuscript. C.D.F. and P.E. contributed to the study design, data interpretation, and critical revision of the manuscript. C.T.-F., R.L., and F.V.-E. contributed to data interpretation and manuscript revision. C.M., L.T., P.B., and F.P. contributed to the experimental work. T.D. and V.M. contributed to cell transfection for overexpression experiments and to manuscript revision. All authors read and approved the final version of the manuscript.

Acknowledgements

The authors thank the Faculty of Medicine and the Graduate School of Universidad Austral de Chile for their support.

References

1. Siegel RL, Kratzer TB, Giaquinto AN, Sung H, Jemal A. Cancer statistics, 2025. CA A Cancer J Clinicians [Internet]. 2025 [cited 2025 Nov 26];75:10–45. https://doi.org/10.3322/caac.21871

2. Bray F, Laversanne M, Sung H, Ferlay J, Siegel RL, Soerjomataram I, et al. Global cancer statistics 2022: GLOBOCAN estimates of incidence and mortality worldwide for 36 cancers in 185 countries. CA A Cancer J Clinicians [Internet]. 2024 [cited 2026 Mar 20];74:229–63. https://doi.org/10.3322/caac.21834

3. Dorochowicz M, Krzemienowska-Cebulla A, Matus I, Senat H, Madej A. Navigating Lung Cancer: Exploring Progress and Obstacles - A Comprehensive Review. J Educ Health Sport [Internet]. 2024 [cited 2025 Nov 26];61:87–108. https://doi.org/10.12775/JEHS.2024.61.006

4. Nooreldeen R, Bach H. Current and Future Development in Lung Cancer Diagnosis. IJMS [Internet]. 2021 [cited 2025 Nov 26];22:8661. https://doi.org/10.3390/ijms22168661

5. Sung H, Ferlay J, Siegel RL, Laversanne M, Soerjomataram I, Jemal A, et al. Global Cancer Statistics 2020: GLOBOCAN Estimates of Incidence and Mortality Worldwide for 36 Cancers in 185 Countries. CA A Cancer J Clinicians [Internet]. 2021 [cited 2025 Nov 26];71:209–49. https://doi.org/10.3322/caac.21660

6. Charpidou A, Hardavella G, Boutsikou E, Panagiotou E, Simsek GÖ, Verbeke K, et al. Unravelling the diagnostic pathology and molecular biomarkers in lung cancer. Breathe [Internet]. 2024 [cited 2025 Nov 26];20:230192. https://doi.org/10.1183/20734735.0192-2023

588 7. Lv P, Man S, Xie L, Ma L, Gao W. Pathogenesis and therapeutic strategy in platinum
589 resistance lung cancer. Biochimica et Biophysica Acta (BBA) - Reviews on Cancer
590 [Internet]. 2021 [cited 2025 Nov 26];1876:188577.
591 https://doi.org/10.1016/j.bbcan.2021.188577

592 8. Tang Q, Wang X, Jin H, Mi Y, Liu L, Dong M, et al. Cisplatin-induced ototoxicity:
593 Updates on molecular mechanisms and otoprotective strategies. European Journal of
594 Pharmaceutics and Biopharmaceutics [Internet]. 2021 [cited 2025 Nov 26];163:60–71.
595 https://doi.org/10.1016/j.ejpb.2021.03.008

596 9. Wang L, Zhao X, Fu J, Xu W, Yuan J. The Role of Tumour Metabolism in Cisplatin
597 Resistance. Front Mol Biosci [Internet]. 2021 [cited 2025 Nov 26];8:691795.
598 https://doi.org/10.3389/fmolb.2021.691795

599 10. Meng XN, Jin Y, Yu Y, Bai J, Liu GY, Zhu J, et al. Characterisation of fibronectin-
600 mediated FAK signalling pathways in lung cancer cell migration and invasion. Br J Cancer
601 [Internet]. 2009 [cited 2025 Nov 26];101:327–34. https://doi.org/10.1038/sj.bjc.6605154

602 11. Li X, Yan S, Dai J, Lu Y, Wang Y, Sun M, et al. Human lung epithelial cells A549
603 epithelial-mesenchymal transition induced by PVA/Collagen nanofiber. Colloids and
604 Surfaces B: Biointerfaces [Internet]. 2018 [cited 2025 Nov 26];162:390–7.
605 https://doi.org/10.1016/j.colsurfb.2017.12.010

606 12. Shintani Y, Maeda M, Chaika N, Johnson KR, Wheelock MJ. Collagen I Promotes
607 Epithelial-to-Mesenchymal Transition in Lung Cancer Cells via Transforming Growth
608 Factor–β Signaling. Am J Respir Cell Mol Biol [Internet]. 2008 [cited 2025 Nov 26];38:95–
609 104. https://doi.org/10.1165/rcmb.2007-0071OC

13. Karacosta LG, Anchang B, Ignatiadis N, Kimmey SC, Benson JA, Shrager JB, et al. Mapping lung cancer epithelial–mesenchymal transition states and trajectories with single-cell resolution. Nature Communications. 2019;10:5587. https://doi.org/10.1038/s41467-019-13441-6

14. Yoshimura A, Horinaka M, Yaoi T, Ono H, Itoh K, Yamada T, et al. Epithelial–mesenchymal transition status is a remarkable biomarker for the combination treatment with avutometinib and defactinib in KRAS-mutated non-small cell lung cancer. British Journal of Cancer. 2024;131:361–71. https://doi.org/10.1038/s41416-024-02727-2

15. Stuardo-Parada A, López-Muñoz R, Villarroel-Espindola F, Figueroa CD, Ehrenfeld P. Minireview: functional roles of tissue kallikrein, kinins, and kallikrein-related peptidases in lung cancer. Med Oncol [Internet]. 2023 [cited 2025 Nov 26];40:224. https://doi.org/10.1007/s12032-023-02090-x

16. Brattsand M, Egelrud T. Purification, Molecular Cloning, and Expression of a Human Stratum Corneum Trypsin-like Serine Protease with Possible Function in Desquamation. Journal of Biological Chemistry [Internet]. 1999 [cited 2025 Nov 26];274:30033–40. https://doi.org/10.1074/jbc.274.42.30033

17. Brattsand M, Stefansson K, Lundh C, Haasum Y, Egelrud T. A Proteolytic Cascade of Kallikreins in the Stratum Corneum. Journal of Investigative Dermatology [Internet]. 2005 [cited 2025 Nov 26];124:198–203. https://doi.org/10.1111/j.0022-202X.2004.23547.x

18. Caubet C, Jonca N, Brattsand M, Guerrin M, Bernard D, Schmidt R, et al. Degradation of Corneodesmosome Proteins by Two Serine Proteases of the Kallikrein Family,

631 SCTE/KLK5/hK5 and SCCE/KLK7/hK7. Journal of Investigative Dermatology [Internet].
632 2004 [cited 2025 Nov 26];122:1235–44. https://doi.org/10.1111/j.0022-202X.2004.22512.x

633 19. Lenga Ma Bonda W, Lavergne M, Vasseur V, Brisson L, Roger S, Legras A, et al.
634 Kallikrein-related peptidase 5 contributes to the remodeling and repair of bronchial
635 epithelium. The FASEB Journal [Internet]. 2021 [cited 2025 Nov 26];35:e21838.
636 https://doi.org/10.1096/fj.202002649R

637 20. Győrffy B. Transcriptome-level discovery of survival-associated biomarkers and therapy
638 targets in non-small-cell lung cancer. British J Pharmacology [Internet]. 2024 [cited 2026
639 Apr 15];181:362–74. https://doi.org/10.1111/bph.16257

640 21. Ramón-López A, Escudero-Ortiz V, Carbonell V, Pérez-Ruixo JJ, Valenzuela B.
641 Farmacocinética poblacional de cisplatino aplicada a la personalización de su dosificación
642 en pacientes oncológicos. Farmacia Hospitalaria [Internet]. 2012 [cited 2025 Nov
643 26];36:392–402. https://doi.org/10.1016/j.farma.2011.08.004

644 22. Pfaffl MW. A new mathematical model for relative quantification in real-time RT-PCR.
645 Nucleic Acids Research [Internet]. 2001 [cited 2025 Nov 26];29:45e–45.
646 https://doi.org/10.1093/nar/29.9.e45

647 23. Lu J, Shi Q, Zhang L, Wu J, Lou Y, Qian J, et al. Integrated Transcriptome Analysis
648 Reveals KLK5 and L1CAM Predict Response to Anlotinib in NSCLC at 3rd Line. Front
649 Oncol [Internet]. 2019 [cited 2025 Nov 26];9:886. https://doi.org/10.3389/fonc.2019.00886

650 24. Ma H, Hockla A, Mehner C, Coban M, Papo N, Radisky DC, et al. PRSS3/Mesotrypsin
651 and kallikrein-related peptidase 5 are associated with poor prognosis and contribute to

652 tumor cell invasion and growth in lung adenocarcinoma. Sci Rep [Internet]. 2019 [cited
653 2025 Nov 26];9:1844. https://doi.org/10.1038/s41598-018-38362-0

654 25. Shinoda Y, Kozaki K, Imoto I, Obara W, Tsuda H, Mizutani Y, et al. Association of
655 *KLK5* overexpression with invasiveness of urinary bladder carcinoma cells. Cancer
656 Science [Internet]. 2007 [cited 2025 Nov 26];98:1078–86. https://doi.org/10.1111/j.1349-
657 7006.2007.00495.x

658 26. Alves MG, Kodama MH, Da Silva EZM, Gomes BBM, Da Silva RAA, Vieira GV, et al.
659 Relative expression of KLK5 to LEKTI is associated with aggressiveness of oral squamous
660 cell carcinoma. Translational Oncology [Internet]. 2021 [cited 2025 Nov 26];14:100970.
661 https://doi.org/10.1016/j.tranon.2020.100970

662 27. Mavridis K, Talieri M, Scorilas A. KLK5 gene expression is severely upregulated in
663 androgen-independent prostate cancer cells after treatment with the chemotherapeutic
664 agents docetaxel and mitoxantrone. Biological Chemistry [Internet]. 2010 [cited 2025 Nov
665 26];391. https://doi.org/10.1515/bc.2010.026

666 28. Papachristopoulou G, Talieri M, Scorilas A. Significant alterations in the expression
667 pattern of kallikrein-related peptidase genes KLK4, KLK5 and KLK14 after treatment of
668 breast cancer cells with the chemotherapeutic agents epirubicin, docetaxel and
669 methotrexate. Tumor Biol [Internet]. 2013 [cited 2025 Nov 26];34:369–78.
670 https://doi.org/10.1007/s13277-012-0558-1

671 29. Chang JS, Kim N, Kim J-Y, Do S-I, Cho Y, Kim H-S, et al. Kallikrein 5 overexpression is
672 associated with poor prognosis in uterine cervical cancer. J Gynecol Oncol [Internet]. 2020
673 [cited 2025 Nov 26];31:e78. https://doi.org/10.3802/jgo.2020.31.e78

30. Kryza T, Silva ML, Loessner D, Heuzé-Vourc'h N, Clements JA. The kallikrein-related peptidase family: Dysregulation and functions during cancer progression. Biochimie [Internet]. 2016 [cited 2026 Mar 24];122:283–99. https://doi.org/10.1016/j.biochi.2015.09.002

31. Maeda O, Ando T, Ohmiya N, Ishiguro K, Watanabe O, Miyahara R, et al. Alteration of gene expression and DNA methylation in drug-resistant gastric cancer. Oncology Reports [Internet]. 2014 [cited 2025 Nov 26];31:1883–90. https://doi.org/10.3892/or.2014.3014

32. Shimomura A, Hagiwara T, Yamada K, Yokoi C, Terayama M, Nohara K, et al. Induction of Kallikrein-Related Peptidase 13 and TET2/3 by Anticancer Drugs and Poor Prognosis of Patients with Esophageal Squamous Cell Carcinoma After Preoperative Treatment. Ann Surg Oncol [Internet]. 2024 [cited 2025 Nov 26];31:251–61. https://doi.org/10.1245/s10434-023-14364-9

33. Pampalakis G, Diamandis EP, Sotiropoulou G. The epigenetic basis for the aberrant expression of kallikreins in human cancers. Biological Chemistry [Internet]. 2006 [cited 2025 Nov 26];387. https://doi.org/10.1515/BC.2006.100

34. Chow TF, Crow M, Earle T, El-Said H, Diamandis EP, Yousef GM. Kallikreins as microRNA targets: an *in silico* and experimental-based analysis. bchm [Internet]. 2008 [cited 2025 Nov 26];389:731–8. https://doi.org/10.1515/BC.2008.071

35. Cuttano R, Afanga MK, Bianchi F. MicroRNAs and Drug Resistance in Non-Small Cell Lung Cancer: Where Are We Now and Where Are We Going. Cancers [Internet]. 2022 [cited 2025 Nov 26];14:5731. https://doi.org/10.3390/cancers14235731

695 36. Yin J, Hu W, Pan L, Fu W, Dai L, Jiang Z, et al. let-7 and miR-17 promote self-renewal
696 and drive gefitinib resistance in non-small cell lung cancer. Oncol Rep [Internet]. 2019
697 [cited 2025 Nov 26]; https://doi.org/10.3892/or.2019.7197

698 37. Zhao J, Fu W, Liao H, Dai L, Jiang Z, Pan Y, et al. The regulatory and predictive
699 functions of miR-17 and miR-92 families on cisplatin resistance of non-small cell lung
700 cancer. BMC Cancer [Internet]. 2015 [cited 2025 Nov 26];15:731.
701 https://doi.org/10.1186/s12885-015-1713-z

702 38. Zheng Y, Guo Z, Li Y. Long non-coding RNA prostate cancer-associated transcript 6
703 inhibited gefitinib sensitivity of non-small cell lung cancer by serving as a competing
704 endogenous RNA of miR-326 to up-regulate interferon-alpha receptor 2. Bioengineered
705 [Internet]. 2022 [cited 2025 Nov 26];13:3785–96.
706 https://doi.org/10.1080/21655979.2022.2031416

707 39. Konoshenko M, Lansukhay Y, Krasilnikov S, Laktionov P. MicroRNAs as Predictors of
708 Lung-Cancer Resistance and Sensitivity to Cisplatin. IJMS [Internet]. 2022 [cited 2025 Nov
709 26];23:7594. https://doi.org/10.3390/ijms23147594

710 40. Adamopoulos PG, Kontos CK, Scorilas A. Molecular cloning of novel transcripts of
711 human kallikrein-related peptidases 5, 6, 7, 8 and 9 (KLK5 – KLK9), using Next-generation
712 sequencing. Sci Rep [Internet]. 2017 [cited 2025 Nov 26];7:17299.
713 https://doi.org/10.1038/s41598-017-16269-6

714 41. Kurlender L, Yousef GM, Memari N, Robb J-D, Michael IP, Borgoño C, et al.
715 Differential Expression of a Human Kallikrein 5 *(KLK5)* Splice Variant in Ovarian and

716 Prostate Cancer. Tumor Biol [Internet]. 2004 [cited 2025 Nov 26];25:149–56.
717 https://doi.org/10.1159/000079147

718 42. Kurlender L, Borgono C, Michael IP, Obiezu C, Elliott MB, Yousef GM, et al. A survey
719 of alternative transcripts of human tissue kallikrein genes. Biochimica et Biophysica Acta
720 (BBA) - Reviews on Cancer [Internet]. 2005 [cited 2025 Nov 26];1755:1–14.
721 https://doi.org/10.1016/j.bbcan.2005.02.001

722 43. Dong Y, Kaushal A, Brattsand M, Nicklin J, Clements JA. Differential splicing of KLK5
723 and KLK7 in epithelial ovarian cancer produces novel variants with potential as cancer
724 biomarkers. Clinical Cancer Research. 2003;9:1710–20.

725 44. Borgoño CA, Diamandis EP. The emerging roles of human tissue kallikreins in cancer.
726 Nat Rev Cancer [Internet]. 2004 [cited 2026 Mar 24];4:876–90.
727 https://doi.org/10.1038/nrc1474

728 45. Pampalakis G, Sotiropoulou G. Tissue kallikrein proteolytic cascade pathways in
729 normal physiology and cancer. Biochimica et Biophysica Acta (BBA) - Reviews on Cancer
730 [Internet]. 2007 [cited 2026 Mar 24];1776:22–31.
731 https://doi.org/10.1016/j.bbcan.2007.06.001

732 46. Johnson JJ, Miller DL, Jiang R, Liu Y, Shi Z, Tarwater L, et al. Protease-activated
733 Receptor-2 (PAR-2)-mediated Nf-κB Activation Suppresses Inflammation-associated
734 Tumor Suppressor MicroRNAs in Oral Squamous Cell Carcinoma. Journal of Biological
735 Chemistry [Internet]. 2016 [cited 2025 Nov 26];291:6936–45.
736 https://doi.org/10.1074/jbc.M115.692640

737 47. Oikonomopoulou K, Hansen KK, Saifeddine M, Tea I, Blaber M, Blaber SI, et al.
738 Proteinase-activated Receptors, Targets for Kallikrein Signaling. Journal of Biological
739 Chemistry [Internet]. 2006 [cited 2026 Mar 24];281:32095–112.
740 https://doi.org/10.1074/jbc.M513138200

741 48. Jackman JK, Stockwell A, Choy DF, Xie MM, Lu P, Jia G, et al. Genome-wide
742 association study identifies kallikrein 5 in type 2 inflammation-low asthma. Journal of
743 Allergy and Clinical Immunology [Internet]. 2022 [cited 2025 Nov 26];150:972-978.e7.
744 https://doi.org/10.1016/j.jaci.2022.03.033

745 49. Allgayer H, Mahapatra S, Mishra B, Swain B, Saha S, Khanra S, et al. Epithelial-to-
746 mesenchymal transition (EMT) and cancer metastasis: the status quo of methods and
747 experimental models 2025. Mol Cancer [Internet]. 2025 [cited 2026 Mar 24];24:167.
748 https://doi.org/10.1186/s12943-025-02338-2

749 50. Youssef KK, Nieto MA. Epithelial–mesenchymal transition in tissue repair and
750 degeneration. Nature Reviews Molecular Cell Biology. 2024;
751 https://doi.org/10.1038/s41580-024-00733-z

752 51. Loren P, Saavedra N, Saavedra K, De Godoy Torso N, Visacri MB, Moriel P, et al.
753 Contribution of MicroRNAs in Chemoresistance to Cisplatin in the Top Five Deadliest
754 Cancer: An Updated Review. Front Pharmacol [Internet]. 2022 [cited 2025 Nov
755 26];13:831099. https://doi.org/10.3389/fphar.2022.831099

756 52. Wheelock MJ, Shintani Y, Maeda M, Fukumoto Y, Johnson KR. Cadherin switching.
757 Journal of Cell Science [Internet]. 2008 [cited 2025 Nov 26];121:727–35.
758 https://doi.org/10.1242/jcs.000455

53. Guo S, Skala W, Magdolen V, Brandstetter H, Goettig P. Sweetened kallikrein-related peptidases (KLKs): glycan trees as potential regulators of activation and activity. Biological Chemistry [Internet]. 2014 [cited 2025 Nov 26];395:959–76. https://doi.org/10.1515/hsz-2014-0140

54. Sidiropoulos KG, White NMA, Bui A, Ding Q, Boulos P, Pampalakis G, et al. Kallikrein-related peptidase 5 induces miRNA-mediated anti-oncogenic pathways in breast cancer. Oncoscience [Internet]. 2014 [cited 2025 Nov 26];1:709–24. https://doi.org/10.18632/oncoscience.91

55. Wang H, Wei X, Zhang D, Li W, Hu Y. Lncap-AI prostate cancer cell line establishment by Flutamide and androgen-free environment to promote cell adherent. BMC Mol and Cell Biol [Internet]. 2022 [cited 2025 Nov 26];23:51. https://doi.org/10.1186/s12860-022-00453-2

56. Wu J-L, Xu C-F, Yang X-H, Wang M-S. Fibronectin promotes tumor progression through integrin αvβ3/PI3K/AKT/SOX2 signaling in non-small cell lung cancer. Heliyon [Internet]. 2023 [cited 2025 Nov 26];9:e20185. https://doi.org/10.1016/j.heliyon.2023.e20185

57. Kakkad S, Krishnamachary B, Fackche N, Garner M, Brock M, Huang P, et al. Collagen 1 Fiber Volume Predicts for Recurrence of Stage 1 Non-Small Cell Lung Cancer. Tomography [Internet]. 2024 [cited 2025 Nov 26];10:1099–112. https://doi.org/10.3390/tomography10070083

58. Yan Y, Du C, Duan X, Yao X, Wan J, Jiang Z, et al. Inhibiting collagen I production and tumor cell colonization in the lung via miR-29a-3p loading of exosome-/liposome-based

781 nanovesicles. Acta Pharmaceutica Sinica B [Internet]. 2022 [cited 2025 Nov 26];12:939–
782 51. https://doi.org/10.1016/j.apsb.2021.08.011

783 59. Zhou F, Sun J, Ye L, Jiang T, Li W, Su C, et al. Fibronectin promotes tumor
784 angiogenesis and progression of non-small-cell lung cancer by elevating WISP3
785 expression via FAK/MAPK/ HIF-1α axis and activating wnt signaling pathway. Exp Hematol
786 Oncol [Internet]. 2023 [cited 2025 Nov 26];12:61. https://doi.org/10.1186/s40164-023-
787 00419-w

788 60. Jiang R, Shi Z, Johnson JJ, Liu Y, Stack MS. Kallikrein-5 Promotes Cleavage of
789 Desmoglein-1 and Loss of Cell-Cell Cohesion in Oral Squamous Cell Carcinoma. J Biol
790 Chem [Internet]. 2011 [cited 2025 Nov 26];286:9127–35.
791 https://doi.org/10.1074/jbc.M110.191361

792 61. De Veer SJ, Swedberg JE, Akcan M, Rosengren KJ, Brattsand M, Craik DJ, et al.
793 Engineered protease inhibitors based on sunflower trypsin inhibitor-1 (SFTI-1) provide
794 insights into the role of sequence and conformation in Laskowski mechanism inhibition.
795 Biochemical Journal [Internet]. 2015 [cited 2025 Nov 26];469:243–53.
796 https://doi.org/10.1042/BJ20150412

797 62. De Veer SJ, Swedberg JE, Brattsand M, Clements JA, Harris JM. Exploring the active
798 site binding specificity of kallikrein-related peptidase 5 (KLK5) guides the design of new
799 peptide substrates and inhibitors. Biological Chemistry [Internet]. 2016 [cited 2025 Nov
800 26];397:1237–49. https://doi.org/10.1515/hsz-2016-0112

801 63. Chavarria-Smith J, Mitchell C, Ho A, Dela Cruz C, Kim J, Demehri S, et al. Dual
802 antibody inhibition of KLK5 and KLK7 for Netherton syndrome and atopic dermatitis.

Science Translational Medicine. 2022;14:eabp9159.
https://doi.org/10.1126/scitranslmed.abp9159

Figure legends

Figure 1. **Kaplan–Meier Plotter survival analysis curves of KLK5 gene expression in non-small cell lung carcinoma.** Kaplan–Meier survival curves comparing low and high KLK5 gene expression in (a–b) non-small cell lung cancer (NSCLC), (c–d) lung adenocarcinoma (LUAD), and (e–f) lung squamous cell carcinoma (SCC). Patients were stratified according to the median KLK5 gene expression level. The number in parentheses (N) indicates the number of patients in each group. Hazard ratios (HRs), confidence intervals (CIs), and log-rank *P*-values are shown in each panel. Statistical significance was defined as $P < 0.05$. Abbreviations: HR, hazard ratio; CI, confidence interval; LUAD, lung adenocarcinoma; SCC, squamous cell carcinoma; NSCLC, non-small cell lung cancer; PFS, progression-free survival; OS, overall survival.

Figure 2. **KLK5 gene expression and protein levels in different A549 lung cancer cell clones.** KLK5 gene expression was quantified by qPCR using the 2^–ΔCt method. Clone 1 (High-KLK5), clone 7 (Low-KLK5), and the empty vector control (Ev) were selected for analysis (**a**). KLK5 expression differences were maintained across four cell passages (**b**). KLK5 protein levels were measured by sandwich ELISA in cell extracts (**c**) and conditioned media (**d**) from wild-type (Wt), Ev, Low-KLK5, and High-KLK5 cells. Data were analyzed using one-way ANOVA followed by Tukey's post hoc test. *p<0.05, **p<0.01, ****p<0.0001 (n=3).

Figure 3. **Estimation of cell proliferation rate in A549 cells.** The effect of recombinant KLK5 (rKLK5) on the proliferation of A549 cells and A549-derived clones was evaluated

using the CellTiter-Glo assay. Cells were cultured in media supplemented with either 1% or 10% FBS and stimulated with rKLK5 at increasing concentrations (20, 50, and 100 ng/mL). Cell proliferation was measured after 24 h. Data was analyzed using one-way ANOVA. n.s., not significant (n=3). In panels (**a**) and (**b**), A549-derived clones were analyzed. In panels (**c**) and (**d**), wild-type A549 cells were stimulated with rKLK5 at 0, 20, 50, and 100 ng/mL.

Figure 4. **Effect of cisplatin on KLK5 expression levels.** KLK5 gene expression was quantified by qPCR using the 2^–ΔCt method (**a**), and protein levels were measured by sandwich ELISA (**b**). Immunofluorescence analysis shows KLK5 localization after 48 h of cisplatin treatment, in the absence or presence of Brefeldin A (BFA). Nuclei were stained with DAPI (blue), and KLK5 is shown in red. Cells were seeded on coverslips and treated with cisplatin for 48 h, with BFA added during the last 3 h of treatment (**c**). Data was analyzed using *t*-test. ***p*<0.01; n.s., not significant (n=3).

Figure 5. **Cell viability following cisplatin treatment in A549 clones.** Dose–response curves after 48 h of cisplatin treatment were determined by MTT assay (**a**), and representative crystal violet staining images are shown in (**b**). Untreated cells served as controls. Dose–response curves were fitted by nonlinear regression using a log (cisplatin concentration) versus normalized response model to estimate IC_{50} values. Statistical comparisons between groups were performed using two-way ANOVA followed by Tukey's multiple-comparison test. n.s., not significant (n= 3).

Figure 6. **KLK5 promotes A549 cell migration.** A549 cell migration was assessed using Transwell inserts (8.0 µm pore size) after overnight incubation. Inserts were fixed and stained with crystal violet, and migrated cells were counted under ×100 magnification. On

the left, representative images of the stained transwells for quantifying migrating cells across different experimental approaches are shown, and on the right, the graph of the quantification results for the different tests. The High-KLK5 clone exhibited increased migration compared to wild-type (Wt) and empty vector (Ev) controls (**a**). In addition, A549 cells stimulated with recombinant KLK5 (rKLK5) at 100 ng/mL showed enhanced migration compared to 0 and 20 ng/mL (**b**). Data were analyzed using one-way ANOVA followed by Tukey's post hoc test. *$p < 0.05$, **$p < 0.01$ ($n = 3$).

Figure 7. **Expression analysis of EMT markers in A549 clones.** EMT marker expression was assessed at the mRNA and protein levels. Relative gene expression of E-cadherin, N-cadherin, and vimentin was determined by qPCR using the 2^–ΔCt method (**a**). Protein expression was evaluated by Western blotting (**b**) and normalized to GAPDH. Molecular weights: E-cadherin, 135 kDa; N-cadherin, 140 kDa; vimentin, 57 kDa; GAPDH, 36 kDa. Data were analyzed using one-way ANOVA followed by Tukey's post hoc test. *$p<0.05$; n.s., not significant ($n=3$).

Figure 8. **Expression of EMT markers in A549 lung cancer cells following rKLK5 stimulation.** Expression levels of E-cadherin, N-cadherin, and vimentin were assessed by qPCR using the 2^–Ct method (**a**), and by Western blot analysis (**b**), normalized to GAPDH. Molecular weights: E-cadherin, 135 kDa; N-cadherin, 140 kDa; vimentin, 57 kDa; GAPDH, 36 kDa. Data was analyzed using one-way ANOVA. n.s., not significant ($n=3$).

Figure 9. **Effect of KLK5 on cell adhesion to extracellular matrix components.** Adhesion of A549 was assessed after 90 minutes of incubation in serum-free medium. The High-KLK5 clone exhibited significantly greater adhesion to collagen I compared to empty

vector (**a**). Stimulation with recombinant KLK5 increased A549 cell adhesion to both fibronectin and collagen I (**b**). Data was analyzed using *t*-test. *$p<0.05$ (n=3).

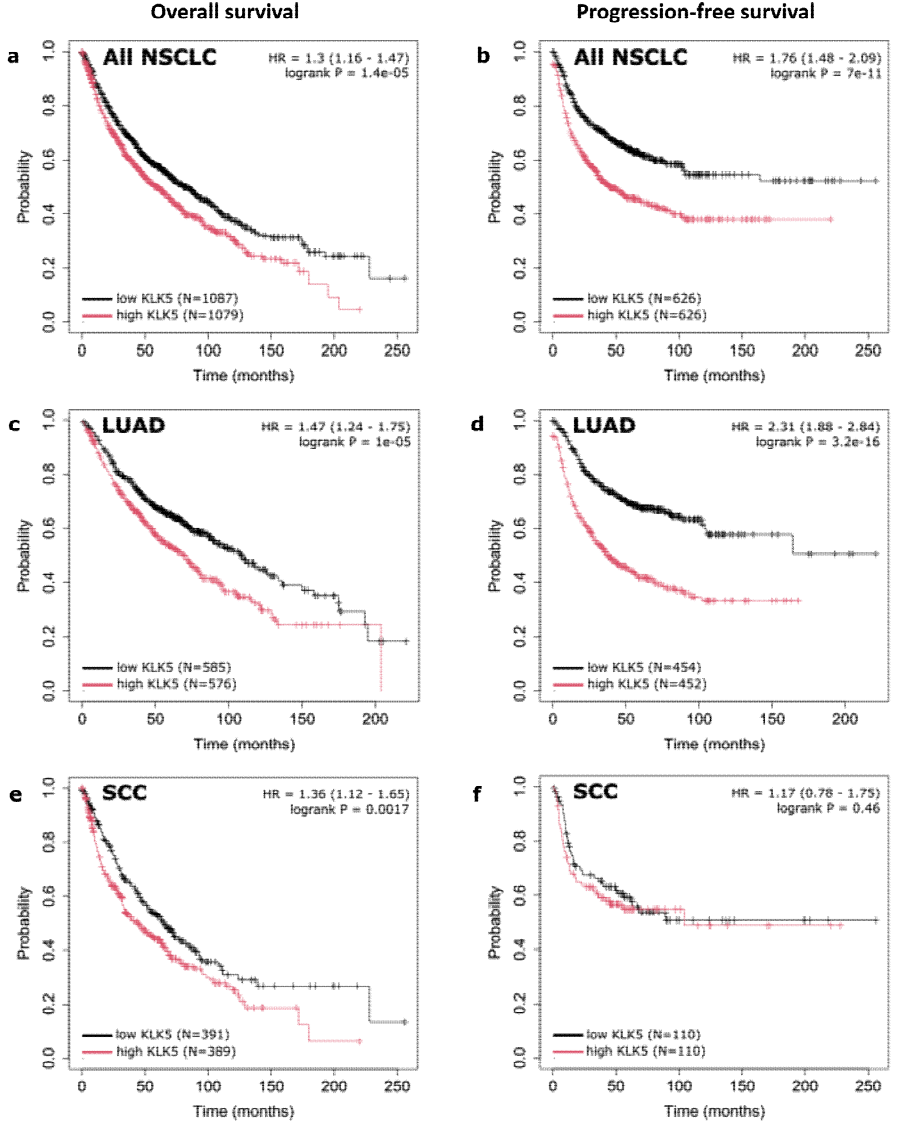


Figure 1. **Kaplan–Meier Plotter survival analysis curves of KLK5 gene expression in non-small cell lung carcinoma.** Kaplan–Meier survival curves comparing low and high KLK5 gene expression in **(a–b)** non-small cell lung cancer (NSCLC), **(c–d)** lung adenocarcinoma (LUAD), and **(e–f)** lung squamous cell carcinoma (SCC). Patients were stratified according to the median KLK5 gene expression level. The number in parentheses (N) indicates the number of patients in each group. Hazard ratios (HRs), confidence intervals (CIs), and log-rank *P*-values are shown in each panel. Statistical significance was defined as $P < 0.05$. Abbreviations: HR, hazard ratio; CI, confidence interval; LUAD, lung adenocarcinoma; SCC, squamous cell carcinoma; NSCLC, non-small cell lung cancer; PFS, progression-free survival; OS, overall survival.

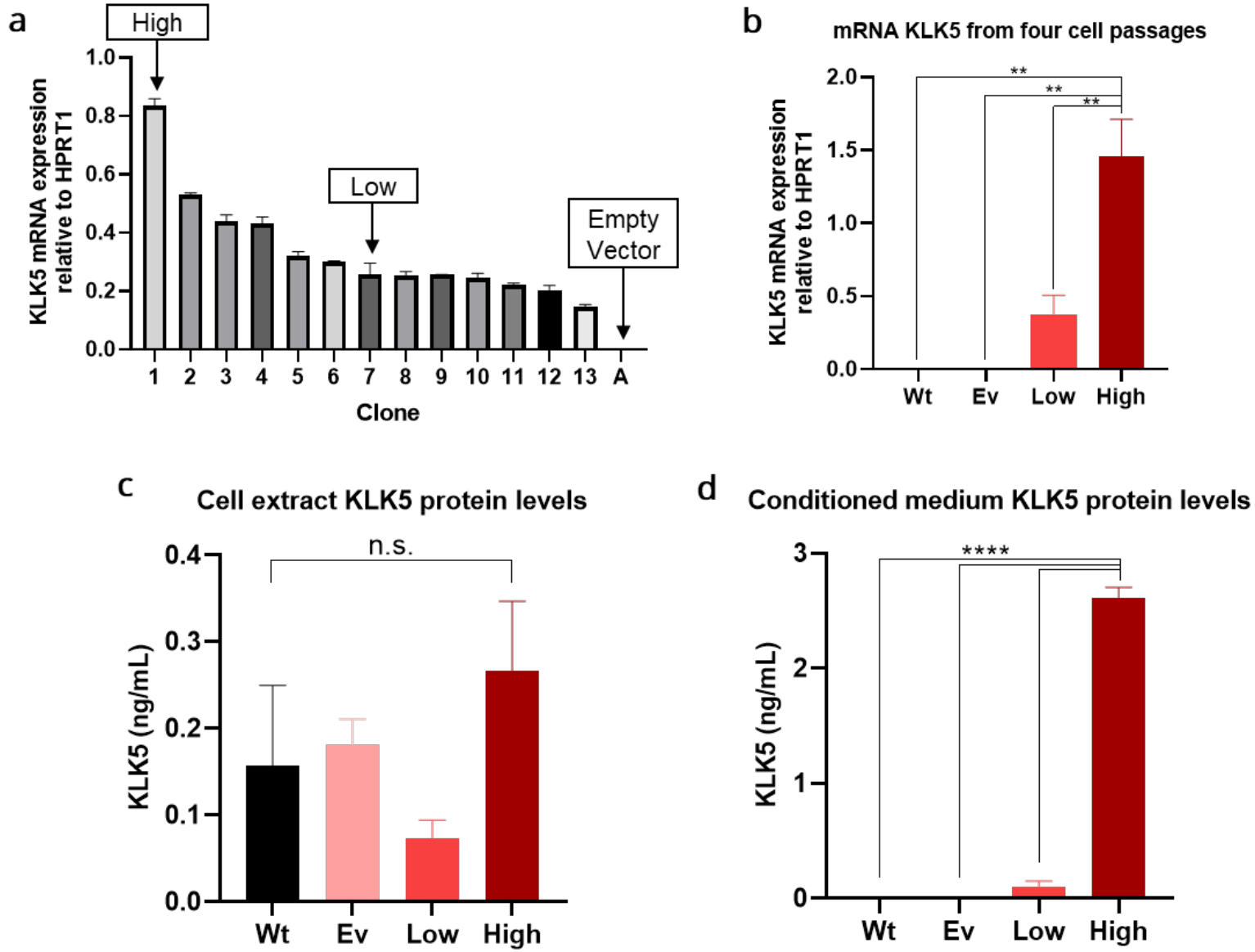


Figure 2. **KLK5 gene expression and protein levels in different A549 lung cancer cell clones.** KLK5 gene expression was quantified by qPCR using the 2^–ΔCt method. Clone 1 (High-KLK5), clone 7 (Low-KLK5), and the empty vector control (Ev) were selected for analysis (**a**). KLK5 expression differences were maintained across four cell passages (**b**). KLK5 protein levels were measured by sandwich ELISA in cell extracts (**c**) and conditioned media (**d**) from wild-type (Wt), Ev, Low-KLK5, and High-KLK5 cells. Data were analyzed using one-way ANOVA followed by Tukey's post hoc test. *p<0.05, **p<0.01, ****p<0.0001 (n=3).

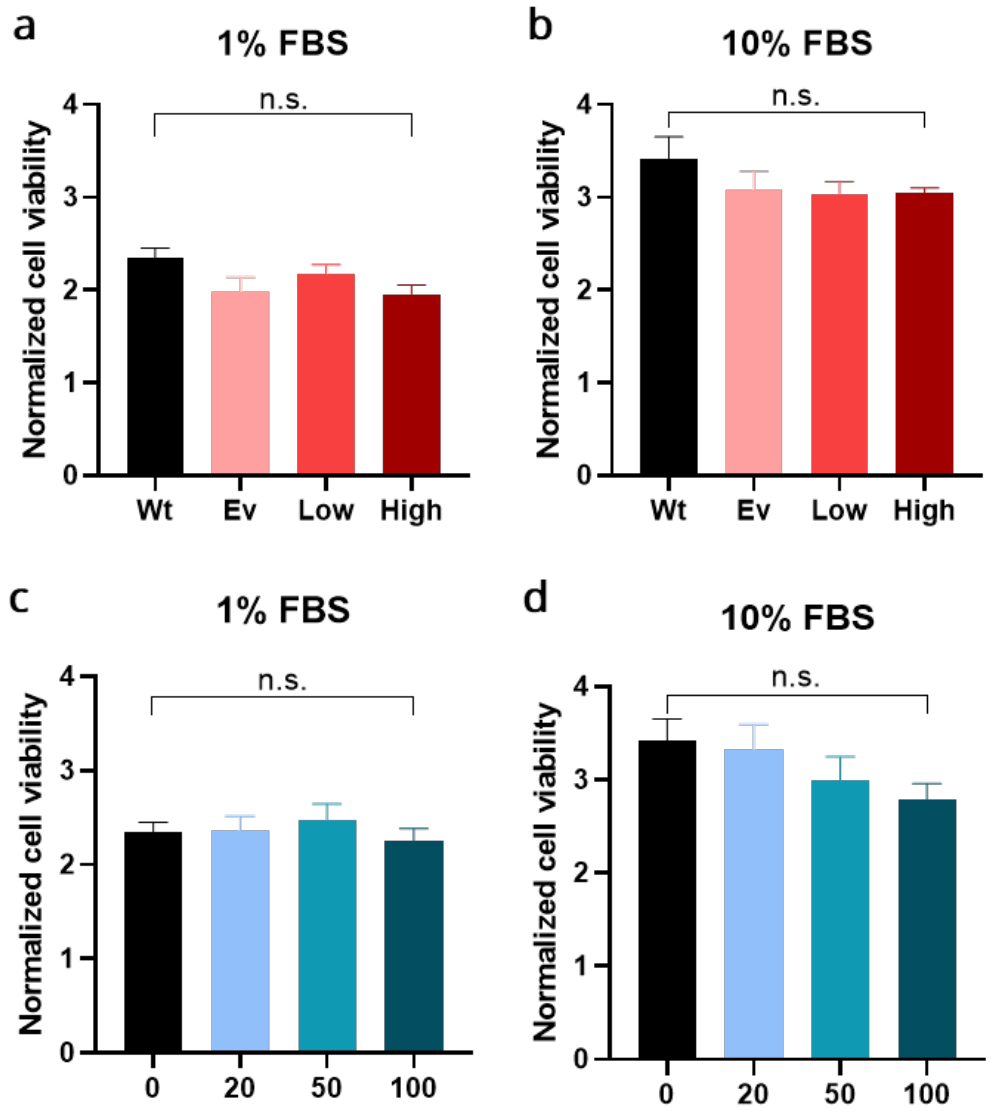


Figure 3. **Estimation of cell proliferation rate in A549 cells.** The effect of recombinant KLK5 (rKLK5) on the proliferation of A549 cells and A549-derived clones was evaluated using the CellTiter-Glo assay. Cells were cultured in media supplemented with either 1% or 10% FBS and stimulated with rKLK5 at increasing concentrations (20, 50, and 100 ng/mL). Cell proliferation was measured after 24 h. Data were analyzed using one-way ANOVA. n.s., not significant (n=3). In panels (**a**) and (**b**), A549-derived clones were analyzed. In panels (**c**) and (**d**), wild-type A549 cells were stimulated with rKLK5 at 0, 20, 50, and 100 ng/mL.

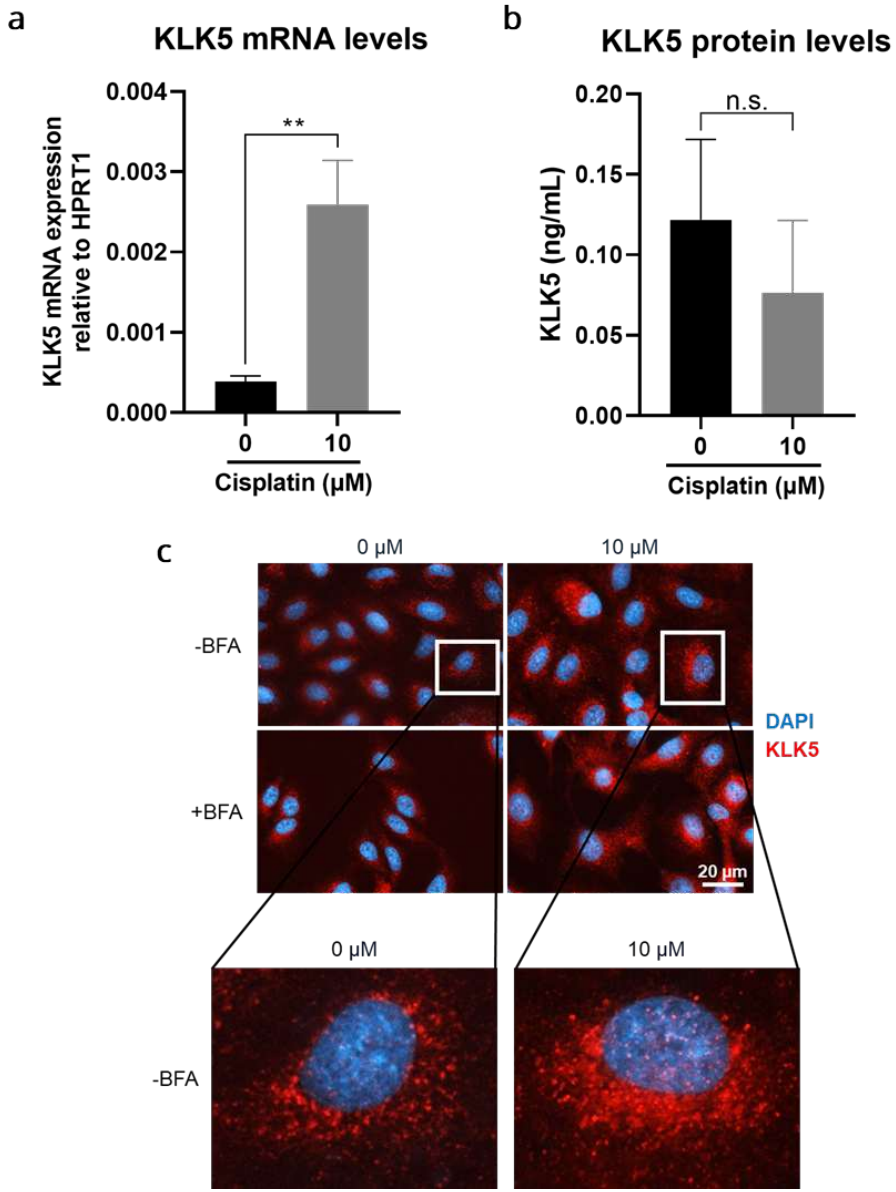


Figure 4. **Effect of cisplatin on KLK5 expression levels.** KLK5 gene expression was quantified by qPCR using the 2^–ΔCt method (**a**), and protein levels were measured by sandwich ELISA (**b**). Immunofluorescence analysis shows KLK5 localization after 48 h of cisplatin treatment, in the absence or presence of Brefeldin A (BFA). Nuclei were stained with DAPI (blue), and KLK5 is shown in red. Cells were seeded on coverslips and treated with cisplatin for 48 h, with BFA added during the last 3 h of treatment (**c**). Data were analyzed using *t*-test. ***p*<0.01; n.s., not significant (n=3).

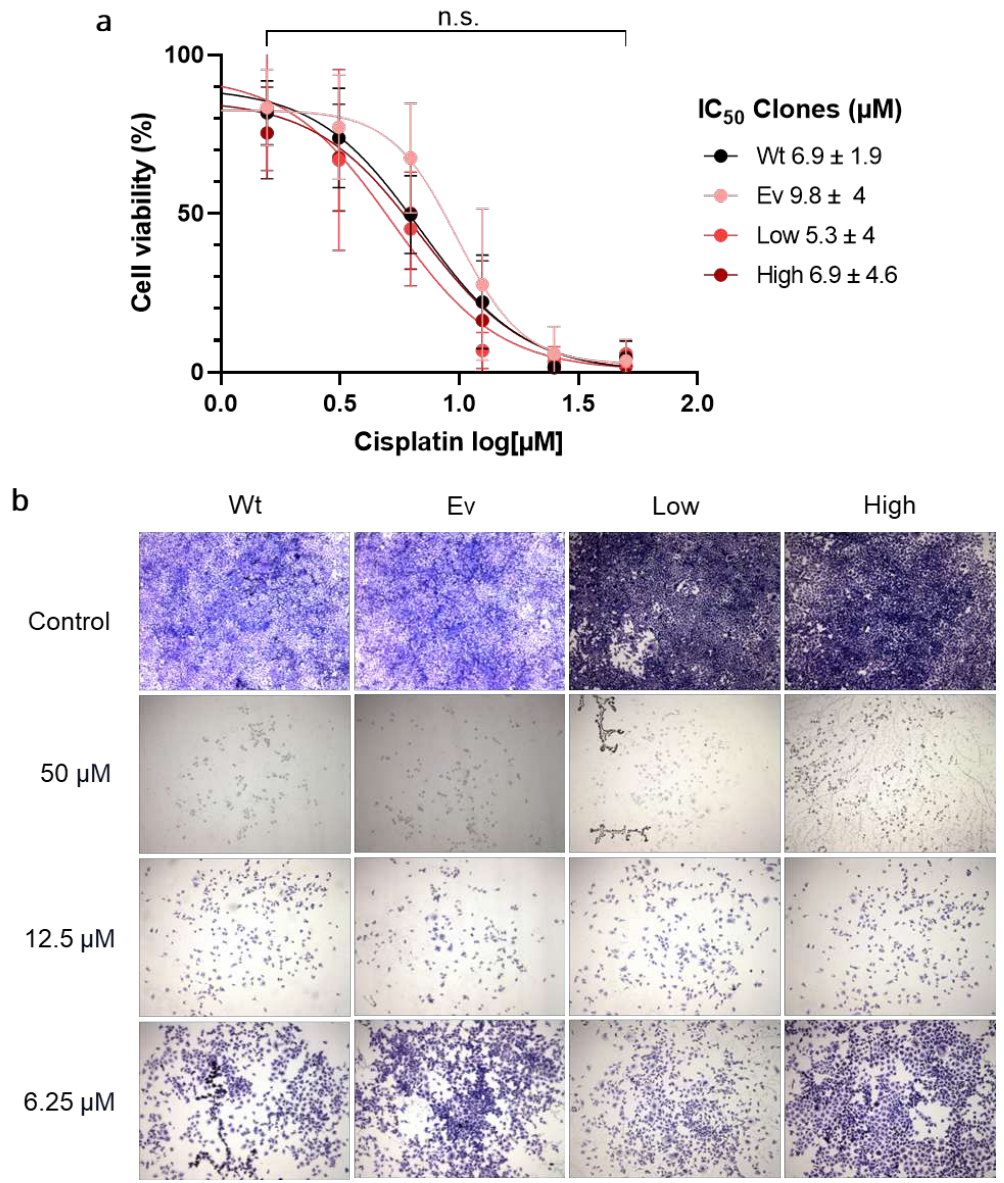


Figure 5. **Cell viability following cisplatin treatment in A549 clones.** Dose–response curves after 48 h of cisplatin treatment were determined by MTT assay (**a**), and representative crystal violet staining images are shown in (**b**). Untreated cells served as controls. Dose–response curves were fitted by nonlinear regression using a log(cisplatin concentration) versus normalized response model to estimate IC_{50} values. Statistical comparisons between groups were performed using two-way ANOVA followed by Tukey's multiple-comparison test. n.s., not significant (n= 3).

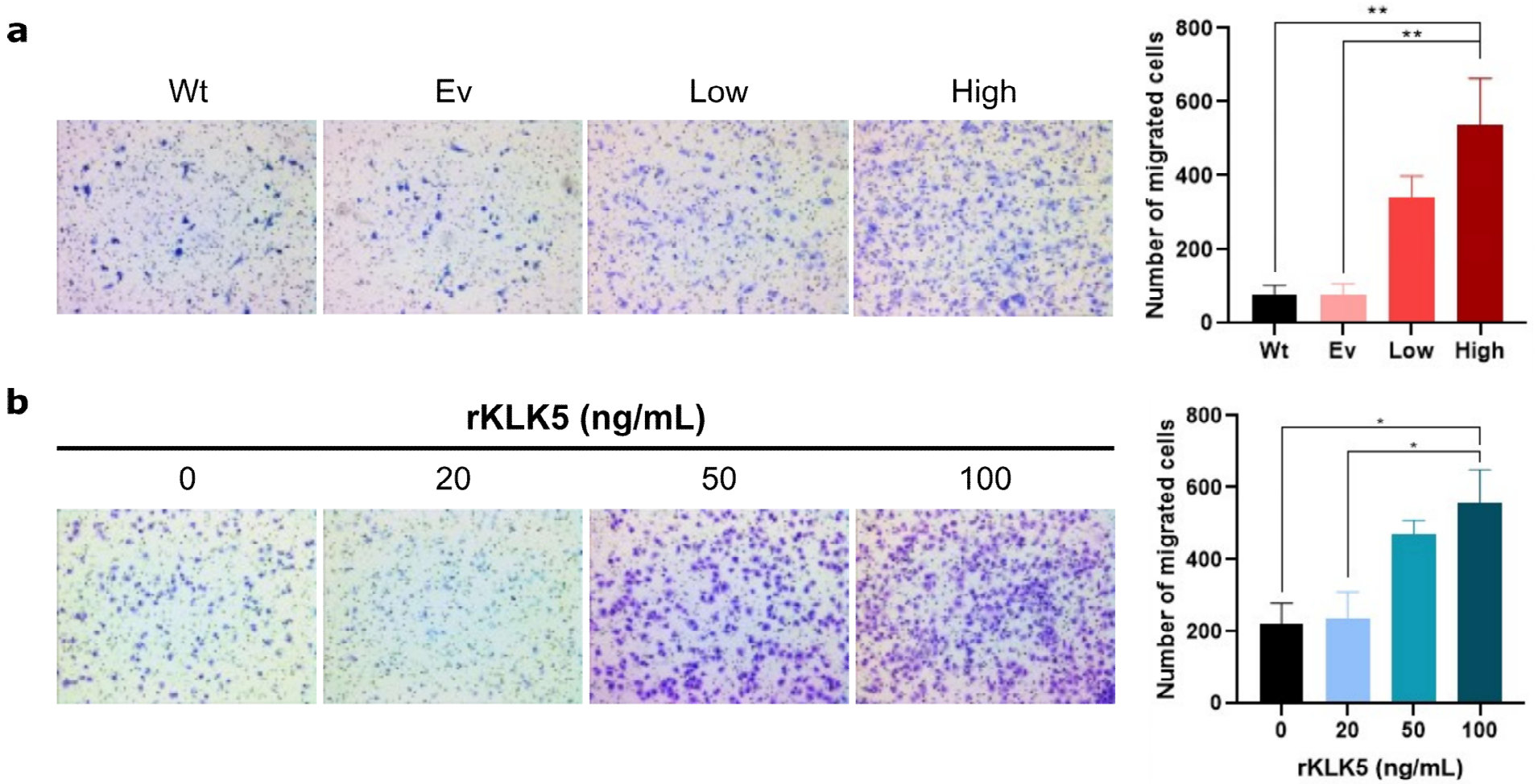


Figure 6. **KLK5 promotes A549 cell migration.** A549 cell migration was assessed using Transwell inserts (8.0 µm pore size) after overnight incubation. Inserts were fixed and stained with crystal violet, and migrated cells were counted under ×100 magnification. On the left side, representative images of the stained transwells for quantification of migrating cells in their different experimental approaches are shown, and on the right, the graph of the quantification of the different tests. The High-KLK5 clone exhibited increased migration compared to wild-type (Wt) and empty vector (Ev) controls (**a**). In addition, A549 cells stimulated with recombinant KLK5 (rKLK5) at 100 ng/mL showed enhanced migration compared to 0 and 20 ng/mL (**b**). Data were analyzed using one-way ANOVA followed by Tukey's post hoc test. *$p < 0.05$, **$p < 0.01$ ($n = 3$).

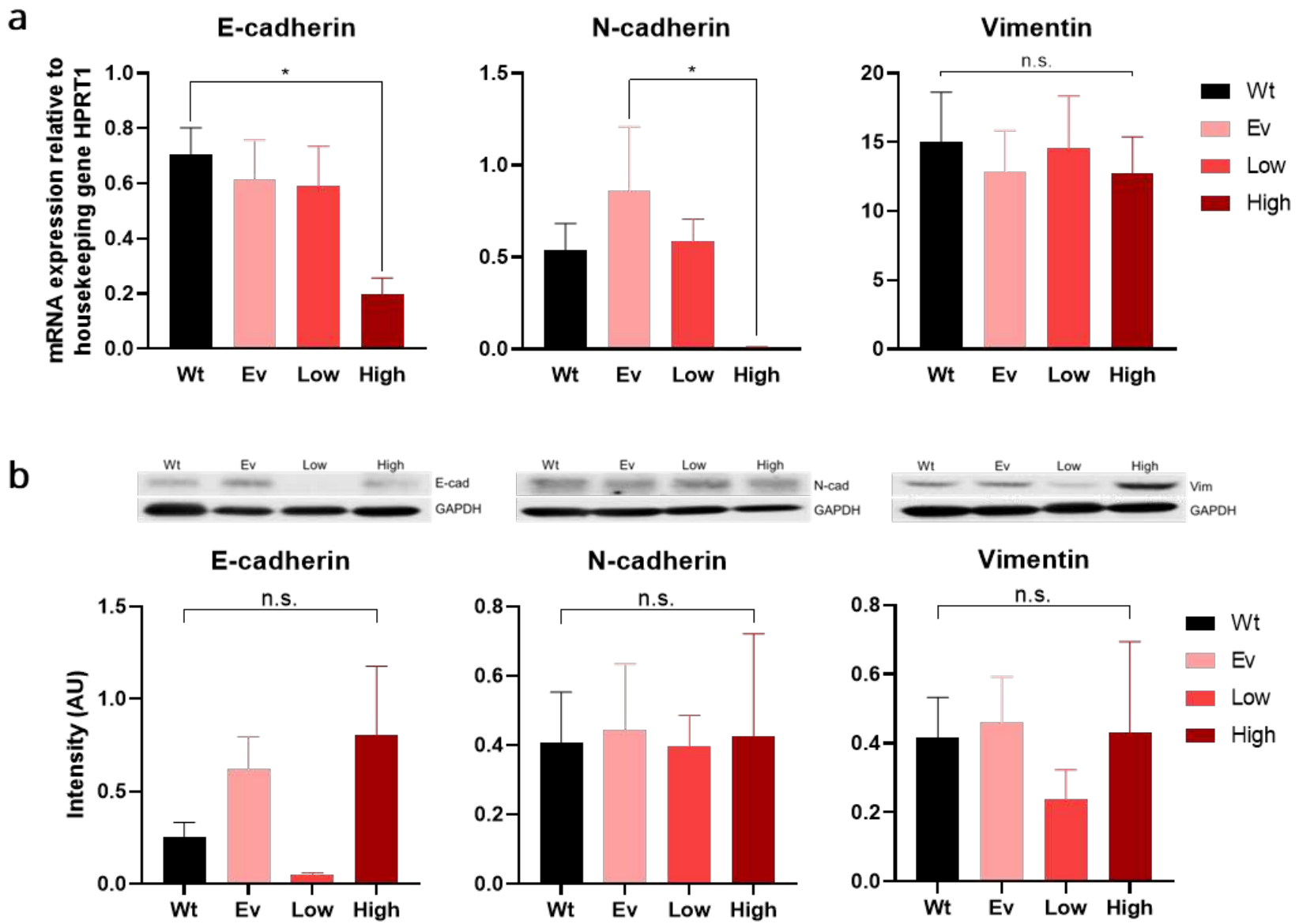


Figure 7. **Expression analysis of EMT markers in A549 clones.** EMT marker expression was assessed at the mRNA and protein levels. Relative gene expression of E-cadherin, N-cadherin, and vimentin was determined by qPCR using the 2^–ΔCt method (**a**). Proteins expression was evaluated by Western blotting (**b**) and normalized to GAPDH. Molecular weights: E-cadherin, 135 kDa; N-cadherin, 140 kDa; vimentin, 57 kDa; GAPDH, 36 kDa. Data were analyzed using one-way ANOVA followed by Tukey's post hoc test. *p<0.05; n.s., not significant (n=3).

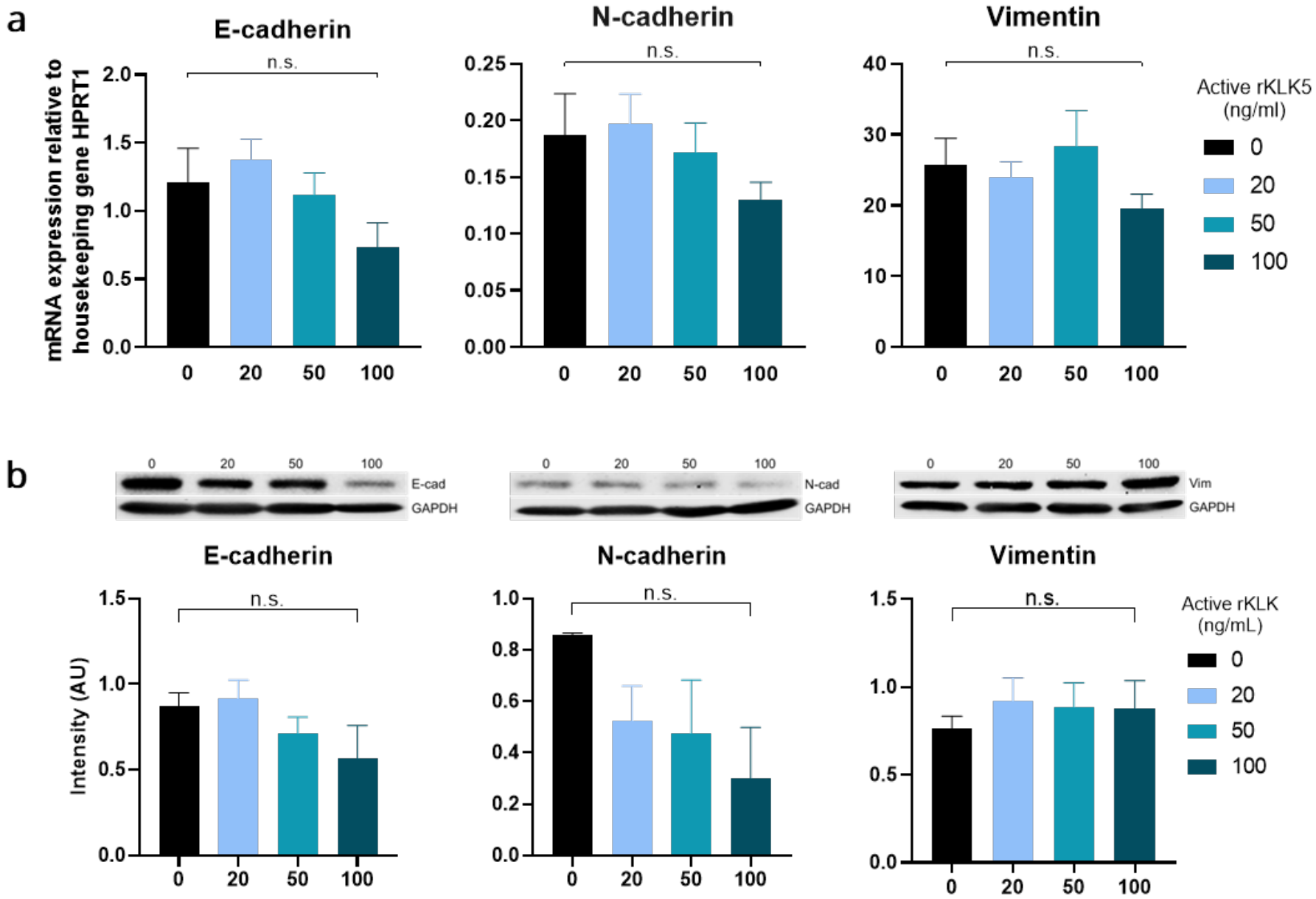


Figure 8. **Expression of EMT markers in A549 lung cancer cells following rKLK5 stimulation.** Expression levels of E-cadherin, N-cadherin, and vimentin were assessed by qPCR using the 2^–Ct method (**a**), and by Western blot analysis (**b**), normalized to GAPDH. Molecular weights: E-cadherin, 135 kDa; N-cadherin, 140 kDa; vimentin, 57 kDa; GAPDH, 36 kDa. Data were analyzed using one-way ANOVA. n.s., not significant (n=3).

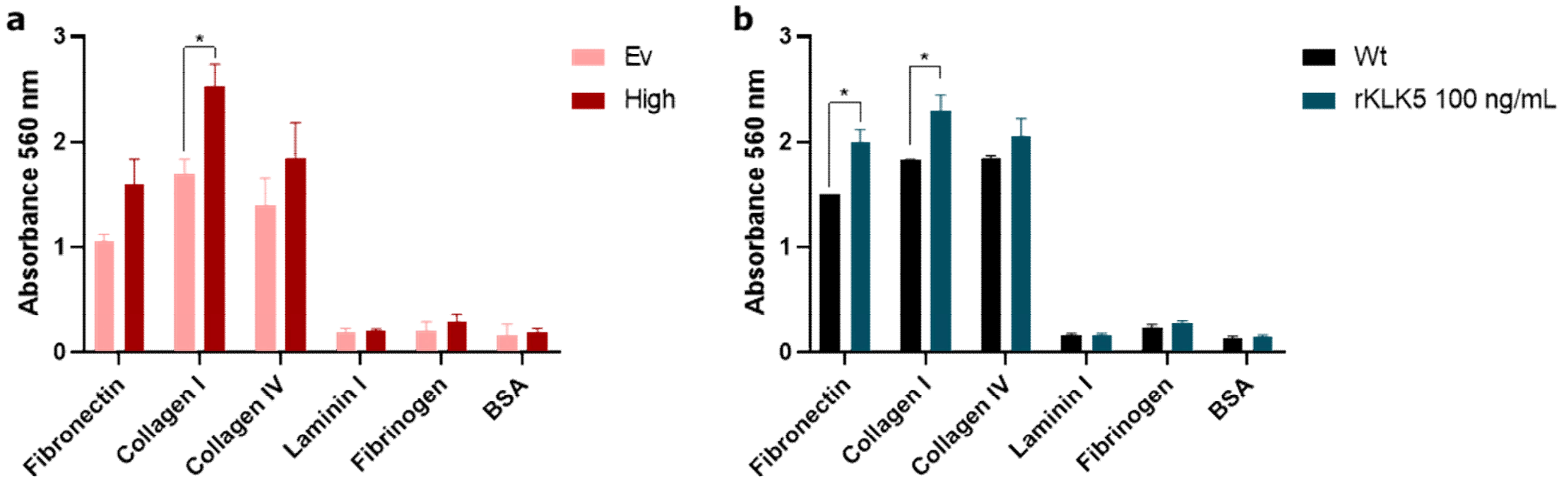


Figure 9. **Effect of KLK5 on cell adhesion to extracellular matrix components.** Adhesion of A549 was assessed after 90 minutes of incubation in serum-free medium. The High-KLK5 clone exhibited significantly greater adhesion to collagen I compared to empty vector (**a**). Stimulation with recombinant KLK5 increased A549 cell adhesion to both fibronectin and collagen I (**b**). Data were analyzed using *t*-test. *$p<0.05$ (n=3).

Supplementary Files

This is a list of supplementary files associated with this preprint. Click to download.

- Supplementaryfigure.pptx